Synchrotron-based spectroscopy for solar energy conversion

F. J. Himpsel*[a], P. L. Cook[b], I. Zegkinoglou[a], Idris Boukahil[a], R. Qiao[c], W. Yang[c], S. C. Pemmaraju[d], D. Prendergast[d], C. X. Kronawitter[e], M. G. Kibria[f], Zetian Mi[f], L. Vayssieres[g]

[a] Dept. of Physics, Univ. of Wisconsin Madison, 1150 University Ave., Madison, WI USA 53706; [b] Natural Sciences Department, Univ. of Wisconsin Superior, Superior, WI USA 54880; [c] Advanced Light Source, Lawrence Berkeley National Laboratory, Berkeley, CA USA 94720; [d] The Molecular Foundry, Lawrence Berkeley National Laboratory, Berkeley, CA USA 94720; [e] Dept. of Chemical and Biological Engineering, Princeton University, Princeton, NJ USA 08544; [f] Dept. of Electrical and Computer Engineering, McGill University, Montreal Canada; [g] Int. Research Center for Renewable Energy, School of Energy&Power Engineering, Xian Jiaotong Univ., Xian PR China 710049

ABSTRACT

X-rays from synchrotron radiation enable incisive spectroscopic techniques which speed up the discovery of new materials for photovoltaics and photoelectrochemistry. A particularly useful method is X-ray absorption spectroscopy (XAS), which probes empty electronic states. XAS is element- and bond-specific, with the additional capability of determining the bond orientation. Close feedback from density functional calculations makes it possible to discover and exploit systematic trends in the electronic properties. Case studies are presented, such as solar cells that combine an absorber with an electron donor and an acceptor in one molecular complex and nanowire arrays serving as photoanodes for water splitting. In addition to the energy levels the lifetimes of the charge carriers play an essential role in device performance. A new generation of laser-like X-ray sources will make it possible to follow the fate of excited charge carriers traveling across a molecular complex or through a device structure in real time.

Keywords: Photovoltaics, water splitting, photoanodes, nanowires, spectroscopy, synchrotron radiation, XAS, XPS

1. INTRODUCTION

In order to systematically develop new materials for enhancing the efficiency of solar energy conversion it is crucial to know their electronic structure. That implies having experimental techniques available for mapping out the electronic states. Concurrent calculations of the energy levels and the associated orbitals provide insight into chemical trends. This feedback helps designing new materials with tailored electronic properties. Ideally one could use photoemission to map out occupied electronic states [1] and inverse photoemission for unoccupied states [2]. They provide the complete information about electronic states in crystalline solids, i.e., their energy and momentum. Photoemission has been widely used for this purpose. But inverse photoemission [3] suffers from a very low cross section (typically 10^{-8} photons per electron). That requires long integration times and degrades the energy resolution to 0.2 - 0.6 eV. Another option is two-photon photoemission, which uses a pump-probe scheme to populate empty states and then probes them by photoemission [4]. It achieves good energy resolution and delivers extra information about the time evolution of excited electrons. But it favors long-lived intermediate states and thus does not provide a complete picture.

The complexity of the materials used in solar energy conversion devices calls for techniques that are element- and bond-specific. These capabilities are provided by spectroscopic methods involving the characteristic core levels of the elements. X-ray Photoelectron Spectroscopy (XPS) determines the binding energy of core levels, X-ray Absorption Spectroscopy (XAS) maps out unoccupied valence levels, and X-ray Emission Spectroscopy (XES) measures occupied valence levels. A combination of XAS and XES named Resonant Inelastic X-ray Scattering (RIXS) probes excitations of an electrons from occupied to unoccupied levels. XAS is rather straightforward to implement by detecting the Total Electron Yield (TEY) or the Total Fluorescence Yield (TFY), as long as there is a tunable synchrotron radiation light source available. A specific atom in a well-defined oxidation state can be selected by the choice of the core level and its chemical shift, as illustrated on the left side of Figure 1. Each peak in the XAS spectrum is then characterized by an optical transition from a specific core level to a specific unoccupied orbital located at that atom.

*fhimpsel@wisc.edu; phone 1 606 263-5590; fax 1 608 265-2334; https://www.physics.wisc.edu/~himpsel/

Solar Hydrogen and Nanotechnology X, edited by Shaohua Shen, Proc. of SPIE Vol. 9560, 95600G · © 2015 SPIE · CCC code: 0277-786X/15/$18 · doi: 10.1117/12.2187038

2. X-RAY ABSORPTION SPECTROSCOPY (XAS)

In the following, the capabilities of XAS for determining the electronic structure of solar energy conversion devices will be illustrated in more detail. Beyond its chemical selectivity this technique is also able to detect the orientation of bond orbitals and to vary the probing depth, as shown in Figure 2.

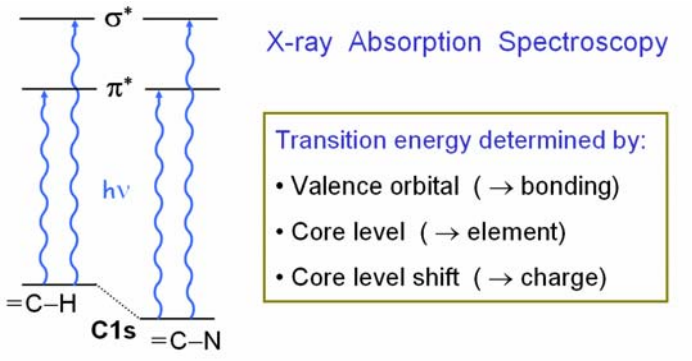

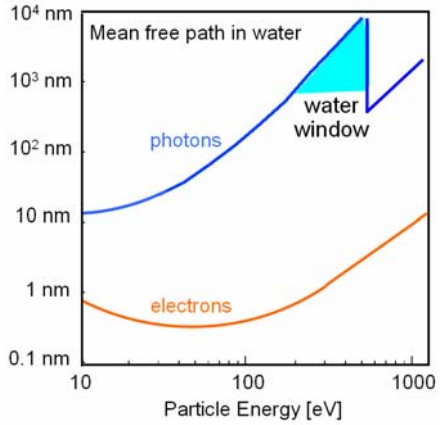

Figure 1. Left: Schematic energy level diagram for X-ray Absorption Spectroscopy (XAS). The photon energy hν is scanned across transitions between core levels and valence states. The electronic structure of a typical organic molecule contains various chemically-shifted C 1s core levels, together with several unoccupied π* and σ* orbitals. The transition energy is determined by three factors which make XAS highly selective to the chemical environment of an atom.

Right: The probing depth of the two principal detection modes in XAS, illustrated qualitatively for water. The Total Electron Yield (TEY) mode collects mainly secondary electrons with about 0-10 eV kinetic energy, while the Total Fluorescence Yield (TFY) mode collects core level fluorescence photons with energies about 10 eV below an absorption edge (here the O 1s edge). The TEY mode probes the surface (≈nm), while the TFY mode probes the bulk (≈μm).

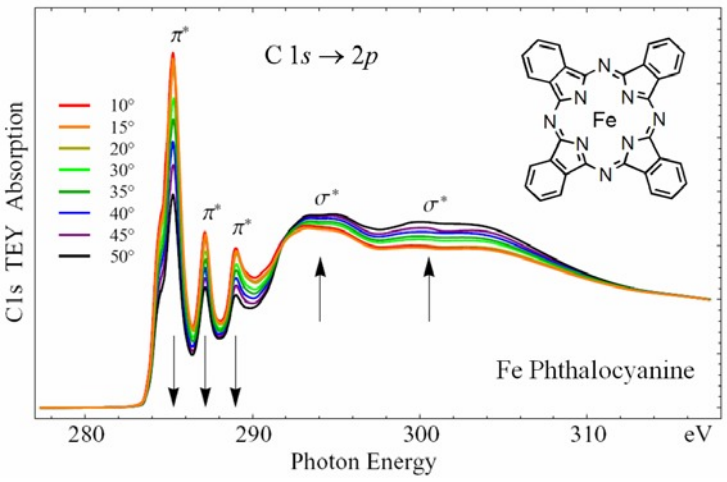

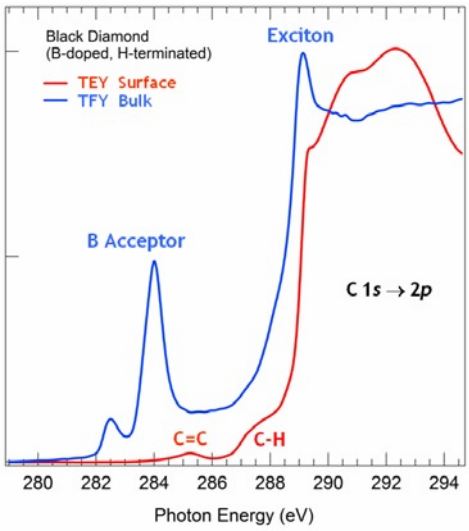

Figure 2. Left: Illustration of the energy level diagram in Fig. 1 by the C 1s XAS spectra of Fe-phthalocyanine, a dye molecule for solar cells (after [5]). For this partially-oriented thin film, the peaks associated with π* and σ* orbitals have opposite polarization dependence, as indicated by arrows. That reflects the orthogonal orientation of the π and σ orbitals in a planar π–system. The π* transitions usually lie below the σ* transitions due to the smaller π–π* splitting.

Right: Varying the probing depth by detecting electrons versus photons. This is demonstrated by a pair of C 1s absorption spectra from H-terminated, B-doped diamond (after [6]). These were obtained simultaneously by measuring the sample current and the X-ray fluorescence (compare the right side of Fig. 1). The bulk-sensitive TFY spectrum shows a bulk exciton at 289 eV (just below the conduction band edge), together with the empty B acceptor level (excited from C in bulk diamond and C next to B). The surface-sensitive TEY spectrum reveals a C–H bond orbital and graphitic C=C defects.

The probing depth of XAS is determined by the mean free paths of the electrons and X-rays, which are shown schematically on the right side of Fig. 1 for an aqueous environment, such as an electrolyte. Electron mean free paths are tabulated in [7], while X-ray attenuation lengths can be obtained from the online CXRO data base [8]. With electron detection one typically obtains probing depths of about a nanometer. Total electron yield detection probes a few nm deep due to the longer mean free path of secondary electrons below 10 eV kinetic energy. These dominate the spectrum of the emitted electrons. By suppressing electrons below 10 eV electrostatically one can reduce the probing depth to a fraction of a nm (often labeled partial electron yield detection). The photon mean free path is of the order of μm in the soft X-ray region. It exhibits sawtooth behavior, dipping down into the submicron regime just above an absorption edge, as shown for the O 1s edge of water in Fig 1. Far from any absorption edge it can reach hundreds of μm. This leads to the peculiar phenomenon of saturation for TFY detection with thick samples. In that situation the mean free path of the emitted photons (with energies just below an absorption edge) becomes larger than that of the absorbed photons (with energies just above the absorption edge). Consequently the escape probability of the emitted photons approaches unity, and the fluorescence yield becomes nearly independent of the absorption depth. As a result the strong absorption peaks become clipped in the XAS spectrum. Therefore, TFY detection is mainly applicable to thin films (thinner than the attenuation length) or to dilute species in thick samples. Since one can measure TEY and TFY simultaneously with different detectors, it is possible to probe both surface and bulk in the same scan. This is illustrated for a H-terminated diamond sample on the right side of Fig. 2 (from [6]). Both spectra exhibit the onset of transitions into the conduction band at 209 eV. The TEY spectrum reveals the C–H bond orbitals at the surface and the π* orbital of graphitic surface defects, while the TFY spectrum detects the core exciton of bulk diamond [9] and the empty B acceptor state. (The double-peak structure of the latter is due to different C 1s binding energies for C in bulk diamond and C next to a B dopant [6].)

The ability of polarization-dependent XAS to detect the orientation of bond orbitals is demonstrated on the left side of Fig. 2. It is a consequence of optical dipole selection rules. These are particularly simple for $s \rightarrow p$ transitions, such as the $1s \rightarrow 2p$ transition in organic molecules. The absorption cross section follows a $\cos^2\theta$ pattern, where θ is the angle between the polarization vector and the axis of the $2p$ valence orbital [10]. For $p \rightarrow s, d$ transitions the selection rules become less strict, but one can still observe substantial polarization dependence and evaluate it quantitatively (for example at the S $2p$ edge of thiophene, a molecule used in organic photovoltaics [11]).

In order to obtain the best possible chemical sensitivity one needs to select the sharpest core levels of the elements. Figure 3 lists them together with their binding energies. They follow a systematic trend with increasing atomic number, as indicated on the left of Fig. 3: These are the filled shells with the highest quantum numbers nl. While all of them are accessible to XPS, the XAS cross section decreases dramatically at threshold for higher angular momentum l, such as d and f. Therefore it is advisable to reduce the listed nl for elements with high atomic numbers (for example from 3d to 2p). That also increases the fluorescence yield relative to the electron yield, which in turn enhances the sensitivity to dilute species (impurities, dopants) by selecting the characteristic fluorescence of the desired element (for example by a filter, an energy-dispersive silicon drift detector, or a grating spectrograph).

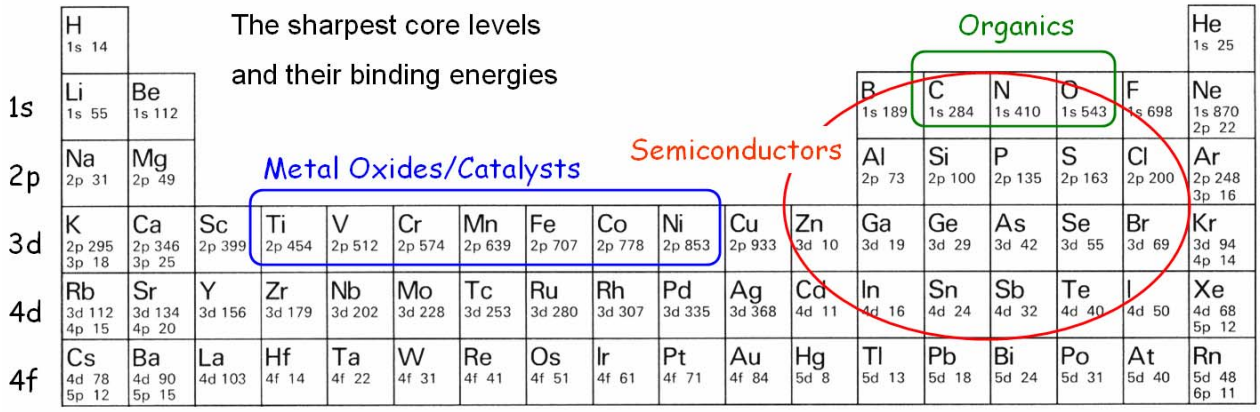

Figure 3. The sharpest core level of each element, together with its binding energy. The column on the left indicates the sequence of these levels with increasing atomic number. The three highlighted groups of elements are relevant to the materials discussed in this article, such as TiO_2, Fe_2O_3, GaN, diamond, and organic dye molecules. Core level lifetime broadening determines the ultimate limit for the chemical sensitivity of XAS and XPS.

3. DONOR-ABSORBER-ACCEPTOR COMPLEXES

As example for an application of XAS to photovoltaics we choose an organic Donor-π-Acceptor (D-π-A) complex, where the three basic elements of a solar cell are combined with atomic precision [12]. These are the electron donor (= hole transport layer), the electron acceptor (= electron transport layer), and the photon absorber (which is a π-system in organic photovoltaics). Such complex achieved a record efficiency for dye-sensitized solar cells [13]. As shown in Figure 4, the absorber is a Zn-porphyrin dye, functionalized by three triphenylamine electron donors and a carboxyl linker for attaching the molecule to TiO_2 nanoparticles as electron acceptors. The N 1*s* absorption edge is particularly informative for such a complex organic molecule, since it contains only two inequivalent N atoms – those in the donor groups and in the porphyrin absorber. At the C 1*s* edge one has to deal with a large number of C atoms which produce a complicated π* manifold that is difficult to unravel. Only the π* transition of the carboxyl linker stands out, since it is shifted to higher photon energy by the chemical shift of the C 1*s* level (not shown). The donor orbital (peak D) can easily be distinguished from the three π*−orbitals of the absorber at lower energies. Those include the lowest unoccupied molecular orbital (labeled π). This assignment is obtained via XAS spectra from the components of the molecular complex, such as the π-A complex (top curve) and the donor (bottom curve). The assignment is confirmed by first-principles calculations [12] (not shown). These also provide the wave functions of the orbitals, whose location inside the molecular complex is relevant to the transport of photoexcited electrons.

In this case, theory not only reproduced the data, but it also helped identifying a problem with the synthesis. In the first batch, the XAS spectrum of the π-A complex contained an extra feature at low energy (second curve from the top in Fig. 4). Calculations traced this feature to porphyrins that lacked the central Zn atom. After improving the synthesis the top spectrum was obtained, which shows exclusively Zn-porphyrin. This results represents a promising initial step in providing feedback from spectroscopy and theory for improving the synthesis of new materials for solar cells.

Density functional calculations are well-suited for explaining trends in the observed electronic structure, such as the peaks observed in XAS. In addition to the core hole binding energy and the energy of the excited valence electron one has to take into account their electron-hole interaction [14]. Encouraged by the predictive power of calculations for the D-π-A complex, one can ask whether it is possible to design new molecules with desirable properties. This was tried recently with the goal of connecting two porphyrin dye molecules by a molecular wire into a tandem architecture that covers a larger part of the solar spectrum efficiently [15]. After screening thousands of differently-functionalized porphyrins, molecular complexes with energy levels appropriate for a tandem architecture were selected.

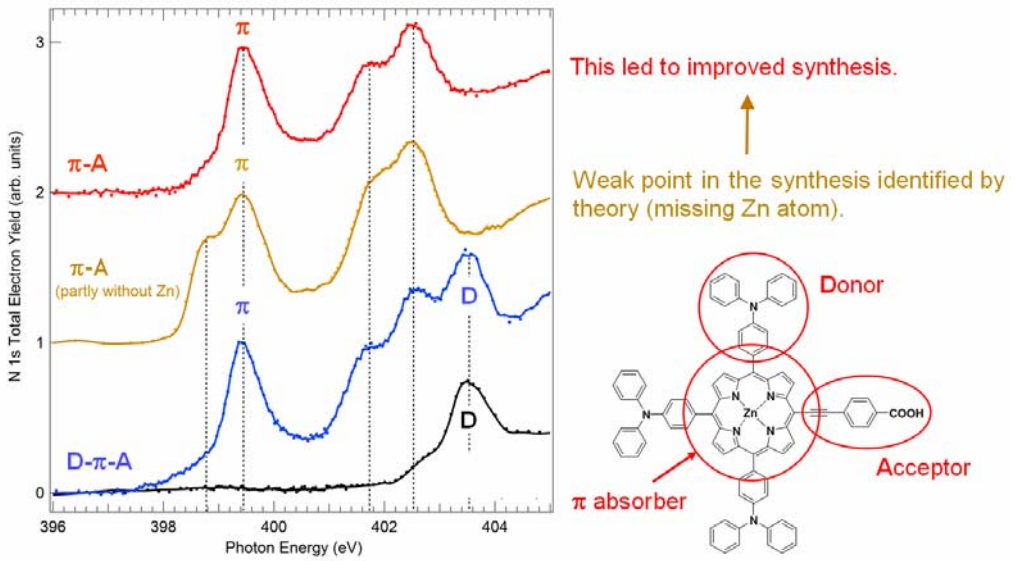

Figure 4. Identification of specific N atoms and their valence orbitals inside a Donor-π-Acceptor (D-π-A) complex via XAS at the N 1*s* edge (after [12]). The amine nirogen in the electron donor gives rise to the orbital labeled D, while the π-bonded nitrogen in the porphyrin absorber produces the orbital labeled π. The assignments were made using reference molecules and confirmed by first-principles calculations. These results provided feedback for the synthesis of this molecular complex.

4. NANOWIRE PHOTOANODES

Artificial photosynthesis has been a long-time goal for producing fuel from sunlight as a complement to the solar electricity provided by photovoltaics [16]. Obtaining conventional fuels by reducing CO_2 would fit into the established fuel infrastructure. But the ultimate challenge remains splitting water into H_2 and O_2 and recombining them in a fuel cell, thereby eliminating carbon from the cycle altogether. A key part of the process is the photoanode, which uses the energy of an absorbed photon to generate an electron-hole pair in a semiconductor with an electrolyte. The hole is subsequentle injected into an adjacent electrolyte, where it splits H_2O into O_2 and H^+. The electron enters the bulk of the semiconductor and eventually travels through an external electrical circuit to the cathode. Crystalline nanowire arrays are emerging a efficient structures for injecting carriers into an electrolyte, since they provide a huge contact area while keeping the path of the carriers short. If the nanowires are single crystalline, the carrier losses along a wire are reduced dramatically. For driving the charge separation in the correct direction, the doping, band bending, and surface charge all need to have the correct signs. Typical semiconductors are TiO_2, Fe_2O_3 [16]-[19], and more recently GaN [20],[21].

Crystalline GaN nanowire arrays with highly-improved quantum efficiency for solar water splitting were grown recently by MBE [20]. The key to such progress has been the control of the Schottky barrier that is induced by occupied gap states at the interface between p-type GaN and the electrolyte. These complex, nanostructured surfaces were investigated by X-ray absorption spectroscopy at the N 1s and Ga 2p edges in order to explore their electronic structure, and in particular the degree of orientation of Ga- and N-derived orbitals [21]. The results at the N 1s edge demonstrate that there is indeed a preferred orientation of the N 2p orbitals along the [0001] axis of the nanowires (see Fig. 5b). But it only amounts to 24.6% of the single crystal orientation in Fig. 5a. At the Ga 2p edge the nanowires exhibit about twice the polarization dependence (not shown), suggesting that the Ga orbitals of the nanowires are more bulk-like. This strong perturbation of the N-derived orbitals is consistent with a N-termination of the nanowire surfaces (both the $(000\bar{1})$ end faces and the $(10\bar{1}0)$ side faces). This termination not only passivates the nanowire surfaces against corrosion by the electrolyte, it also establishes the correct polarization at the interface to the electrolyte. To detect such a re-orientation of surface orbitals requires the short probing depth of XAS in the TEY mode (here 2 nm). This is a small fraction of the nanowire diameter of 50-75 nm.

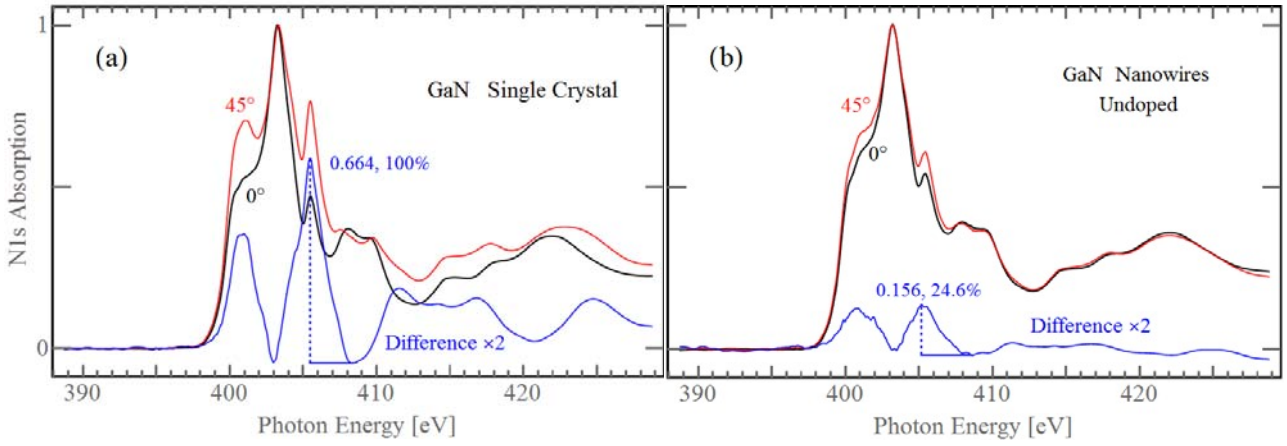

Figure 5. Exploring the empty valence orbitals of GaN nanowire photoanodes via XAS at the N 1s edge (from [21]). The polarization dependence (=difference between 0^o and 45^o angle of incidence) is taken as a quantitative measure of how well the N orbitals are oriented at the surface of the nanowires (24.6% compared to a bulk single crystal). Similar measurements at the Ga 2*p* edge yield a value of 69% (not shown). This is consistent with a N surface termination of the nanowires.

5. OUTLOOK

While energy levels are necessary for characterizing solar cells and photoanodes, they are not sufficient to predict their performance. The other key quantity is the lifetime of the excited charge carriers, which involves a variety of carrier loss mechanisms. Those can be addressed by combining ultrafast time resolution with spectroscopies, such as XAS, XPS, and UPS. Particularly promising is the ability of XPS and XAS to locate specific atoms and in a molecular complex or across a device structure, as demonstrated in Figure 4. Transient absorption or fluorescence techniques with visible/UV/IR lasers are already used in photovoltaics to obtain an overall lifetime. But that represents a conglomerate of

various loss mechanisms with different lifetimes. In order to isolate the bottleneck for efficient carrier collection, it is necessary to resolve the processes that take place in different regions of a device and at various defects. They can be pinpointed by X-ray probes which are able to locate specific atoms in specific bond configurations, such as pump-probe XAS and XPS.

Figure 6 gives an example of the capabilities of time-resolved XAS (from [22]). Dye molecules containing a central Fe atom are pumped with visible light to excite some of the Fe 3*d* valence electrons from the low-spin ground state to a high-spin excited state. This gives rise to an extra transition in the XAS spectrum that is shifted by 1.7 eV from the ground state peak. Another mechanism for detecting excited atoms is a bleaching of ground state transitions caused by de-populating the occupied levels. Performing such experiments at various absorption edges (e.g., Fe 2*p*, N 1*s* and C 1*s*) pinpoints the locations of photo-excited carriers within a molecular complex. From the decay times one finds out where carriers are lost. With existing 3rd generation synchrotron light sources such experiments are still at a "heroic" stage, i.e., it takes a full day to obtain a spectrum. But at the next generation, laser-like X-ray light sources they will become routine. That should make ultrafast XAS experiments highly valuable for a detailed analysis of carrier loss processes in photovoltaic and photoelectrochemical devices.

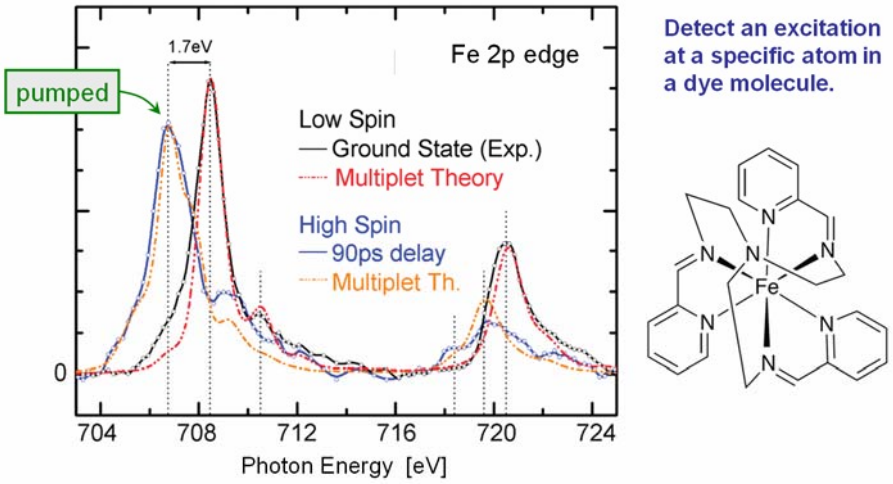

Figure 6. Pump-probe XAS experiment, where carriers are excited at the central Fe atom by a visible (560 nm) pump pulse and probed with soft X-rays after a delay of 90 psec (from [22]). The pump pulse switches the configuration of the Fe 3*d* valence electrons from low spin to high spin. This is inferred via atomic multiplet calculations in the presence of the crystal field (see [23],[24]). Such time-resolved XAS results suggest exciting experiments, where one follows the fate of photo-excited charge carriers in real time as they travel across a molecular complex or through various charge transport layers.

ACKNOWLEDGMENT

The XAS work was supported by the NSF with the awards CHE-1026245 and DMR-1121288 (MRSEC) and by the DOE (BES) under the contracts DE-SC0006931 and DE-AC02-05CH11231 (ALS).

REFERENCES

[1] B. W. D' Andrade, S. Datta, S. R. Forrest, P. Djurovich, E. Polikarpov, M. E. Thompson, "Relationship between the ionization and oxidation potential of molecular organic semiconductors", Organic Electronics 6, 11 (2005).
[2] P. I. Djurovich, E. I. Mayo, S. R. Forrest, M. E. Thompson,"Measurement of the lowest unoccupied molecular orbital energies of molecular organic semiconductors", Organic Electronics **10**, 515 (2009)
[3] F. J. Himpsel, "Inverse photoemission from semiconductors", Surface Science Reports 12, 1 (1990).
[4] T. Fauster, "Two-photon photoelectron spectroscopy", in: Surface and Interface Science. Ed. K. Wandelt, Wiley-VCH (Weinheim) 1, 253 (2012).

[5] Peter L. Cook, Xiaosong Liu, Wanli Yang, and F. J. Himpsel, "X-ray absorption spectroscopy of biomimetic dye molecules for solar cells", J. Chem. Phys. 131, 194701 (2009).
[6] I. Zegkinoglou, P. L. Cook, P. S. Johnson, W. Yang, J. Guo, D. Pickup, R. González-Moreno, C. Rogero, R. E. Ruther, M. L. Rigsby, J. E. Ortega, R. J. Hamers, and F. J. Himpsel, "Electronic Structure of Diamond Surfaces Functionalized by $Ru(tpy)_2$", J. Phys. Chem. C 116, 13877 (2012).
[7] C. J. Powell and A. Jablonski, "NIST Electron Inelastic-Mean-Free-Path Database - Version 1.2", National Institute of Standards and Technology, Gaithersburg, MD (2010): http://www.nist.gov/srd/nist71.cfm
[8] CXRO database for X-ray attenuation lengths (2010): http://henke.lbl.gov/optical_constants/atten2.html
[9] J.F. Morar, F.J. Himpsel, G. Hollinger, G. Hughes, and J.L. Jordan, "Observation of a C-1s Core Excitation in Diamond", Phys. Rev. Lett. 54, 1960 (1985).
[10] Phillip S. Johnson, Changshui Huang, M. Kim, Nathaniel S. Safron, Michael S. Arnold, Bryan M. Wong, Padma Gopalan, and F. J. Himpsel, "Orientation of a Monolayer of Dipolar Molecules on Graphene from X-ray Absorption Spectroscopy", Langmuir 30, 2559 (2014).
[11] Ehren M. Mannebach, Josef W. Spalenka, Phillip S. Johnson, Zhonghou Cai, F. J. Himpsel, Paul G. Evans, "High Hole Mobility and Thickness-Dependent Crystal Structure in α,ω-Dihexylsexithiophene Single-Monolayer Field-Effect Transistors", Adv. Funct. Mater. 23, 554 (2013).
[12] I. Zegkinoglou, Maria-Eleni Ragoussi, S. C. Pemmaraju, P. S. Johnson, D. Pickup, J. E. Ortega, D. Prendergast, Gema de la Torre, F. J. Himpsel, "Spectroscopy of Donor-π-Acceptor Porphyrins for Dye-Sensitized Solar Cells", J. Phys. Chem. C 117, 13357 (2013).
[13] A. Yella, H.-W. Lee, H. N. Tsao, C. Yi, A. K. Chandiran, Md. K. Nazeeruddin, E. Wei-Guang Diau, C.-Y. Yeh, S. M. Zakeeruddin, M. Grätzel, "Porphyrin-Sensitized Solar Cells with Cobalt (II/III)–Based Redox Electrolyte Exceed 12 Percent Efficiency", Science 334, 629 (2011).
[14] J.M. García-Lastra, P. L. Cook, F. J. Himpsel, and A. Rubio, "Communication: Systematic shifts of the lowest unoccupied molecular orbital peak in x-ray absorption for a series of 3d metal porphyrins", J. Chem Phys. 133, 151103 (2010).
[15] Kristian B. Ørnsø, Juan M. Garcia-Lastra, Gema De La Torre, F. J. Himpsel, Angel Rubio, and Kristian S. Thygesen, "Design of two-photon molecular tandem architectures for solar cells by ab initio theory", Chemical Science 6, 3018 (2015).
[16] Y. Tachibana, L. Vayssieres, J. R. Durrant, "Artificial photosynthesis for solar water-splitting", Nature Photonics 6, 511 (2012).
[17] C. X. Kronawitter, I. Zegkinoglou, C. Rogero, J.-H. Guo, S. S. Mao, F. J. Himpsel, L. Vayssieres, "On the interfacial electronic structure origin of efficiency enhancement in Hematite photoanodes", J. Phys. Chem. C 116, 22780 (2012).
[18] C. X. Kronawitter, I. Zegkinoglou, S.-H. Shen, P. Liao, I. S. Cho, O. Zandi, Y.-S. Liu, K. Lashgari, G. Westin, J.-H. Guo, F. J. Himpsel, E. A. Carter, X. L. Zheng, T. W. Hamann, B. E. Koel, S. S. Mao, L. Vayssieres, "Titanium Incorporation into Hematite Photoelectrodes: Theoretical Considerations and Experimental Observations", Energy Environ. Sci. 7, 3100 (2014).
[19] C. X. Kronawitter, Ioannis Zegkinoglou, S. Shen, J.-H. Guo, F. J. Himpsel, S. S. Mao, L. Vayssieres, On the orbital anisotropy in hematite nanorod-based photoanodes, Communication: Phys. Chem. Chem. Phys. 15, 13483 (2013).
[20] M.G. Kibria, S. Zhao, F.A. Chowdhury, Q. Wang, H.P.T. Nguyen, M.L. Trudeau, H. Guo, Z. Mi, "Tuning the surface Fermi level on p-type gallium nitride nanowires for efficient overall water splitting", Nat. Comm. 5:3825 (2014).
[21] R. Qiao, W. Yang, P. S. Johnson, I. Boukahil, Md Kibria, Z. Mi, L. Vayssieres, F. J. Himpsel, "Polarization-dependent X-Ray Absorption Spectroscopy of Oriented GaN Nanowires for Water Splitting", to be submitted.
[22] N. Huse, T. K. Kim, L. Jamula, J. K. McCusker, F. M. F. de Groot, R. W. Schoenlein," Photo-Induced Spin-State Conversion in Solvated Transition Metal Complexes Probed via Time-Resolved Soft X-ray Spectroscopy", JACS 132, 6809 (2010).
[23] E. Stavitski and F. M. de Groot, "The CTM4XAS program for EELS and XAS spectral shape analysis of transition metal L edges", Micron 41, 687 (2010); http://www.anorg.chem.uu.nl/CTM4XAS/
[24] Phillip S. Johnson, J. M. García-Lastra, Colton K. Kennedy, Nathan J. Jersett, Idris Boukahil, F. J. Himpsel, Peter L. Cook, "Crystal fields of porphyrins and phthalocyanines from polarization-dependent 2*p*-to-3*d* multiplets", J. Chem. Phys. 140, 114706 (2014).